Title
FAST SELF-COMPENSATING ELLIPSOMETER

Authors
Mathieu, H.J.
McClure, D.E.
Muller, R.H.

Publication Date
1973-12-01

Submitted to Review of
Scientific Instruments

LBL-2256
Preprint C.1

FAST SELF-COMPENSATING ELLIPSOMETER

H. J. Mathieu, D. E. McClure and R. H. Muller

December 1973

Prepared for the U. S. Atomic Energy Commission
under Contract W-7405-ENG-48

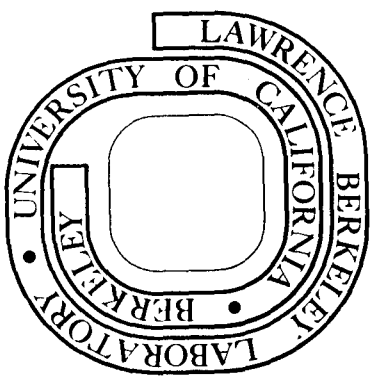

DISCLAIMER

FAST SELF-COMPENSATING ELLIPSOMETER

H. J. Mathieu, D. E. McClure and R. H. Muller

Inorganic Materials Research Division, Lawrence Berkeley Laboratory and
Department of Chemical Engineering; University of California
Berkeley, California 94720

ABSTRACT

A compensating automatic ellipsometer that employs Faraday rotators has been constructed. Speed of response and resolution superior to that of any similar instrument now in use have been achieved through the use of novel Faraday solenoids, modulation with high frequency and large amplitude, and refinements in circuitry.

I. INTRODUCTION

The use of ellipsometers for the observation of surfaces and thin films has greatly increased in recent years. The principal shortcoming of a manually operated ellipsometer is its slow response, since several minutes are required for a high-resolution compensating measurement in one zone. The speed of response can be increased by operation in non-compensating modes[1,2] or by use of a self-compensating instrument.[3] The latter choice is preferable because such instruments record the state of polarization without being influenced by changes in irradiance.

The operation of a self-compensating ellipsometer requires an error signal, that is derived from a modulation of the state of polarization, and is used to drive a control-loop to reach compensation (extinction). Designs of automatic, compensating ellipsometers realized so far employ electro-mechanical modulation and compensation,[4] electro-optic modulation with mechanical compensation,[5] and magneto-optic (Faraday cell) modulation and compensation.[6] The instrument reported here belongs to the last category. Since Faraday rotation over a useful dynamic range of polarizer and analyzer azimuth requires the manipulation of sizeable magnetic fields, the inductance of Faraday coils needs careful consideration. Both an adequate AC modulation amplitude and a fast response of azimuth rotation (to be referred to as DC response) are, in practice, limited by coil inductances.

Desired characteristics of an automatic ellipsometer include fast response, large dynamic range and high resolution.

II. PRINCIPLES OF OPERATION

The operation of the present design is based on suggestions by Winterbottom[7] and a previous construction by Layer.[6] The arrangement of optical components, shown in Fig. 1, provides monochromatic, elliptically polarized light incident on the specimen. At compensation (extinction), the reflected light is linearly polarized. Compensation is reached by effectively rotating the planes of polarization (azimuths) of polarizer and analyzer prisms over the dynamic range by means of two Faraday cells to either side of mechanically established prism azimuths. Current measurement in the Faraday coils serves as (incremental) azimuth readout.

A control (error) signal is derived from a modulation of the Faraday rotation. As indicated in Fig. 2, the photodetector output provides an approximately parabolic transfer curve as a function of polarizer or analyzer azimuth. Thus, phase-sensitive detection and integration of the photodetector signal caused by the azimuth modulation results in an error signal that has a different sign on opposite sides of the minimum and is zero at minimum transmitted irradiance (compensation, null). Analyzer and polarizer azimuths are modulated at the same frequency; their separation is achieved by a difference in phase of exactly 90° between them.[6]

III. FARADAY CELLS

The Faraday rotation θ of the azimuth of linearly polarized light depends on the magnetic field strength H, the length ℓ and the Verdet constant V of the cell core.

$$\theta = H\ell V \tag{1}$$

The magnetic field strength at the axial end of the solenoid is[8]

$$H = \frac{NI}{2\sqrt{\ell^2 + r^2}} \quad . \tag{2}$$

The symbols are identified at the end. The slew-rate S for the self-nulling process, defined as[9]

$$S = \frac{d\theta}{dt} \tag{3}$$

can therefore be formulated as

$$S = a\, N \frac{dI}{dt} \quad , \tag{4}$$

with the constant a defined as

$$a = \frac{V\ell}{2\sqrt{\ell^2 + r^2}} \quad . \tag{5}$$

Since changes in solenoid current, resulting from a compliance voltage E of the power supply, are hindered by the self-inductance L

$$-\frac{dI}{dt} = \frac{E}{L} \quad , \tag{6}$$

Eq. (4) becomes

$$S = -\frac{aNE}{L} \quad . \tag{7}$$

The inductance L of the Faraday solenoid is

$$L = \mu\mu_o \frac{N^2}{\ell} \pi r^2 \quad . \tag{8}$$

The amplitude of the azimuth modulation is given by Eq. (9). Primed quantities refer to the modulating (AC) coil

$$\theta_o = \frac{a' N' E'}{L'} = \frac{S'}{\omega} \quad . \tag{9}$$

With a core of manageable length (chosen to be 152 mm), fairly high magnetic fields have to be generated ($2.9 \cdot 10^3$ A $m^{-1} deg^{-1}$ average over the length of the solenoid) in order to produce the necessary azimuth rotations both, for modulation and compensation. In addition, fast response capabilities of the instrument require low inductance of Faraday solenoids, even with the use of operational amplifier feedback techniques. Also, temperature rise due to power dissipation at continuous service should be kept to a minimum because changes in Verdet constant and birefringence of the core are deleterious.

The present Faraday cell design is illustrated in Fig. 3. It differs from the previously-used design[6] because a single, air-cooled solenoid cannot provide the desired combination of properties.[9] Instead, separate solenoids, as proposed earlier by Winterbottom[7] have been employed to generate modulating (to be referred to as AC) and compensating (to be referred to as DC) fields. In the present construction, these solenoids are concentric and magnetically isolated.

An inner coil (F) of very low inductance (0.01 mH) carries the high frequency (10 kHz) AC signal that results in a ±0.9° azimuth modulation.

This amplitude of modulation, rather than the 0.15° employed previously, has been found necessary for fast response and high resolution in agreement with other authors.[1,10] Also, since the control signal must be derived from an average of at least 5-10 cycles of the AC modulation, the previously-used modulation frequency of 500 Hz cannot provide response times in the range of milliseconds.

A water-cooled outer coil (D) of somewhat higher inductance (1.1 mH) carries the DC current and provides for a large dynamic range (±27°) with fast response. It can carry ±125A continuously with a temperature rise of less than 2°C. Temperature sensors, connected to interlocks, monitor the outlet temperature of the cooling water. The two coils are magnetically separated by a counter-wound third coil (E) that is connected in series with the AC coil. Solenoid characteristics are summarized in Table I.

Computed magnetic field distributions in the Faraday cell core are shown in Fig. 4. Although the axial magnetic field strength varies by about 40% from the center of the coil to its flanges, the radial variation over the central 1.27 cm diameter of the core that determines the uniformity of extinction is at most 0.17%.

An optical glass (Table II) of low absorbance, small residual birefringence and fairly high Verdet constant was chosen for the cell core.[11] The end faces of 152 mm long rods of 19 mm diameter were polished parallel to each other within 1 min and coated with anti-reflecting layers of MgF_2. The rods were also carefully annealed.[12]

IV. CONTROL CIRCUIT

The control circuit is based on similar principles employed previously by Layer.[6] But it employs a much higher modulating frequency and makes extensive use of integrated circuit elements. A block diagram is given in Fig. 5. The azimuth modulation originates from a 10 kHz ozillator[13] O that drives the modulation amplifiers[14] M1 and M2 for analyzer and polarizer, separated by a 90° difference in phase. The gain of these amplifiers can be adjusted manually. A 10A peak-to-peak signal results in a ±0.9° azimuth modulation.

As pointed out in Section III, the slew rate S is mainly determined by the geometry of the Faraday cell. However, application of operational amplifier feedback technique (voltage-to-current converter) improves the slew rate that can be achieved experimentally. Table I shows, that the experimentally determined slew rate S is increased from a theoretically expected value of 1240 deg/s to 1600 deg/s.[21]

The reference signals for the phase-sensitive detectors are derived from the oscillator signals in the following way: A pair of series connected integrated circuit monostable multi-vibrators (TD1, TD2) are used to generate the reference signal in each channel, the first of which is adjustable and is used for phase adjustment. The adjustment range is almost 360° for a 10 kHz signal. The second monostable circuit in each channel is adjusted to form a symmetrical square wave at the reference frequency (SWG1, SWG2). The monostable multivibrator outputs are then buffered through a TTL inverter circuit and fed to the phase synchronous detector inputs (L1, L2).

The modulation in transmitted irradiance is detected by photomultiplier PM.[15] The signal channel follower (F) is a 10× preamplifier connecting an operational amplifier in the "follower-with-gain" position. The tuned amplifier (TA) is an operational amplifier with a band reject feedback network. The circuit is a bandpass amplifier with a bandwidth of about 400 Hz and center frequency 10 kHz. The gain of this stage is approximately 75.

The tuned amplifier feeds the two quadrature detection channels. The first circuit in each channel is a variable gain stage (A1, A2) (adjusted externally). The gain stage is followed by a simple inverting operational amplifier (I1, I2) to provide full wave phase synchronous detection by the full-wave demodulator (L1, L2). This detector is an integrated circuit FET switch with a normally open contact, a normally closed contact and a switch driver circuit within the same package. One side of each contact is connected to become the output of the detector. The detected signal is available on the controller front panel ("Det. Out") for adjusting phase relations[16] in the system in order to avoid cross-modulation between channels (Fig. 6). Also, the switch drive signal is available on the controller front panel ("Ref. Out").

The integrated detector output signal is displayed in a panel meter (used for manual nulling) and fed into an analog integrator (Int1, Int2) with a variable time constant (range 0.001 sec to 0.5 sec) to reduce noise if necessary. The amplifier used in this integrator is a high gain, low drift, low input current offset, low voltage offset unit. The integrator output signal is used to drive the Faraday cell DC-current power supplies (PS1, PS2). The integrator output can be

disconnected from the power supplies (by means of manual switches) during setup or preparation periods and for manual (mechanical) nulling. Under open-loop conditions, the magnet current can be adjusted manually.

The Faraday cell DC-power supplies (PS) are bipolar, operational, current-regulated amplifiers with a current rating of ±125 A (corresponding to ±27° rotation of the plane of polarization with the present Faraday cells) with a compliance voltage of ±12 V. The maximum slewing rate of the supplies with the Faraday cell solenoids is approximately 9 A/msec corresponding to 1.8° azimuth rotation/msec. Operationally (small signal) the power supply and magnet have an approximate bandwidth of 400 Hz.

Each power supply uses a complimentary output stage consisting of banks of water-cooled parallel high power transistors adjusted to zero quiescent current. Current sampling is done with four 20 A-50 mV meter shunts connected in series. Indium foil is used on the shunt interfaces to minimize contact resistance between shunts. Extreme care in layout is necessary in this unit to minimize ripple due to stray fields.

V. READOUT SYSTEM

The readout signals are derived from the current sampling shunts in the DC power supplies. These signals are a measure of the electrical azimuth rotation, to be added to the mechanically established azimuths of polarizer and analyzer prisms. The electrical azimuth rotations are displayed by means of two digital voltmeters that have been calibrated to show the rotation in degrees with a resolution of 0.001°. For continuous recording, particularly of fast changes, the signals are also displayed by a multiple channel light-beam oscillograph[17] with a resolution of 0.0005°. For highest resolution, the output signals can be externally filtered with variable time constants before display. Other experimental parameters are recorded simultaneously on other channels of the oscillograph.

VI. MECHANICAL CONSTRUCTION

Telescopes and azimuth circles of a commercial manual ellipsometer[18] have been used in the present construction. These components have been equipped with facilities for alignment and azimuth adjustment. Together with Faraday cells and light source,[19] the components have been mounted in two sub-assemblies to either side of the specimen. The sub-assemblies, in turn, rest on a rigidly-built table (103×219 cm) with a surface flat to ±25 μm, and allow one to vary the angle of incidence (presently 75°) without re-aligning individual optical components. Figure 6 illustrates the physical arrangement of optical components. Further details of mechanical design can be found elsewhere.[20]

VII. PERFORMANCE

Tests to characterize the performance of automatic ellipsometers have been developed and will be described in detail elsewhere.[21] The tests are based on the use of rotating mirrors for the generation of fast, well-defined changes in the optical properties of a reflecting surface. Performance characteristics thus obtained are summarized in Table III. The range of values given for slew rate and resolution results from the capability to increase resolution at the expense of speed by increasing the integration time from its normal value of about 1 ms. Changes in azimuth smaller than 0.01°, the mechanical resolution of the present azimuth circles, can only be interpreted as relative measurements. The difference in dynamic range of polarizer and analyzer is due to a slight difference in the maximum current output of the two DC power supplies.

VIII. CONCLUSIONS

To our knowledge, the present combination of performance characteristics has not been previously obtained with an automatic ellipsometer that employs Faraday cell rotators. Speed of response and resolution have been obtained through the use of low-inductance Faraday solenoids and a high modulation frequency. The most desirable future improvement of the instrument appears to be an extension of the dynamic range, that could well be tripled by an increase in current capacity of the power supplies and a variation in the solenoid design.

ACKNOWLEDGEMENTS

This work was conducted under the auspices of the U. S. Atomic Energy Commission. One of the authors (H. J. Mathieu) wishes to thank the Deutsche Forschungsgemeinschaft for its financial support. We thank Mr. W. T. Giba for mechanical design and construction.

LIST OF SYMBOLS

a	constant for DC-solenoid $\left(\frac{\text{deg}}{\text{A}}\right)$ (Eq. (5))
a'	constant for AC-solenoid $\left(\frac{\text{deg}}{\text{A}}\right)$ (Eq. (5))
E	voltage applied to DC-solenoid (V)
E'	voltage applied to AC-solenoid (V)
H	magnetic field strength $\left(\frac{\text{A}}{\text{m}}\right)$
I	current (A)
ℓ	length of solenoid (m)
L	self-inductance of DC-solenoid (H)
L'	self-inductance of AC-solenoid (H)
N	number of turns of DC-solenoid
N'	number of turns of AC-solenoid
r	mean radius of DC-solenoid (m)
r'	radius of AC-solenoid (m)
S	slew rate of DC-coil (deg/s)
S'	slew-rate of AC-coil (deg/s)
t	time (s)
V	Verdet constant of Faraday cell core $\left(\frac{\text{deg}}{\text{A}}\right)$
μ	permeability of Faraday cell core $\left(\frac{\text{H}}{\text{m}}\right)$
μ_o	magnetic field constant ($= 1.256 \cdot 10^{-6} \frac{\text{Vs}}{\text{Am}}$)
θ	azimuth rotation due to DC current (deg)
θ_o	amplitude of azimuth modulation due to AC current (deg)
ω	angular frequency of AC modulation (rad/s)

REFERENCES

1. B. D. Cahan and R. F. Spanier, Surf. Sci. 16, 166 (1969).

2. J. Kruger, Corrosion 22, 88 (1966).

3. R. H. Muller in Advances in Electrochemistry and Electrochemical Engineering, Vol. 9, R. H. Muller, ed. (Wiley-Interscience, N. Y., 1973), p. 167.

4. J. L. Ord and B. L. Wills, J. Appl. Opt. 6, 1673 (1967).
J. L. Ord, Surf. Sci. 16, 155 (1969).

5. H. Takasaki, Appl. Opt. 5, 759 (1966).

6. H. P. Layer, Surf. Sci. 16, 177 (1969).

7. A. B. Winterbottom in Ellipsometry in the Measurement of Surfaces and Thin Films, E. Passaglia, R. R. Stromberg and J. Kruger, eds. NBS Misc. Publ. No. 256 (1964), p. 97.

8. This formula represents the magnetic field strength of a solenoid, for which $R<\ell$. The magnetic field strength at the end of the solenoid seems to reach better agreement with experimentally determined values because of the geometry of the solenoid, which is actually built of about seven layers of about 18 turns each.

9. H. J. Mathieu and R. H. Muller, Faraday Cell Solenoids for Automatic Ellipsometers, LBL-1836, U. of Calif., Berkeley, September 1973.

10. C. L. Riddiford, J. Opt. Soc. Am. 63, 1434 (1973).

11. H. Gu, Ellipsometry of Surface Layers (M. S. Thesis), LBL-165, University of California, Berkeley, December 1971.

12. Heated to 400°C in 1 hr, maintained for 1 day, cooled at 1.5°C/h for first 50°, then at 2.5°C/h to room temperature.

13. Oscillator Burr-Brown 4023/24.

14. Amplifiers Bogen C100 (100 W).

15. RCA IP21.

16. H. J. Mathieu, D. E. McClure and R. H. Muller, Self-Compensating Automatic Ellipsometer Manual, LBL-1478, July 1973.

17. Honeywell 1108 Visicorder with M24-350 galvanometers (frequency response 1000 Hz).

18. Gaertner Ellipsometer Model L-119.

19. Short-arc high pressure mercury lamp (Osram HBO 100 W/Z) with IR absorbing filter (Oriel G-776-7100), interference filter for 546±5 nm (Oriel No. 2201) and stabilized power supply (Oriel C-12-20).

20. W. Giba and R. H. Muller, Mechanical Components for Automatic Ellipsometer, LBL-2505, U. of Calif., Berkeley.

21. R. H. Muller and H. J. Mathieu, submitted to Applied Optics.

Table I. Characteristics of Faraday Cell Solenoids

	DC Coil	AC Coil	Separation Coil
Number of turns	131	51.8	5.5
Number of layers	7	1	1
Conductor diam. (cm)	0.6×0.6	0.3	0.2×1.2
Conductor length (m)	$15 \cdot 10^{-2}$	$15 \cdot 10^{-2}$	$15 \cdot 10^{-2}$
Mean solenoid radius (m)	$5 \cdot 10^{-2}$	$1.2 \cdot 10^{-2}$	$3.8 \cdot 10^{-2}$
Applied voltage (V)	12	12	12
Characteristic constant (Eq. (5), deg/A)	$9.27 \cdot 10^{-4}$	$8.92 \cdot 10^{-4}$	$9.04 \cdot 10^{-4}$
Specific azimuth rotation (deg/A)	0.2	0.2	---
Frequency (kHz)	---	10	10
Self-inductance (mH)	1.13	0.01 (calc)	0.001 (calc)
Resistance (Ohm)	0.3	0.01	$0.9 \cdot 10^{-3}$
Slew-rate (deg/s)	1240 (calc) 1600 (meas)	555,999 (calc)	---
Max. azimuth rotation (deg)	±27	±0.90	---

Table II. Properties of Glass for Faraday Cell Core (Schott SF-6)

Refractive index at 546 nm	1.81357
Transmission 25 mm, 546 nm	0.996
Verdet constant (deg/A)	2.0×10^{-3}
Density (g/cm^3)	5.18
Expansion coefficient (deg^{-1})	8.1×10^{-6}

Table III. Performance Characteristics of Automatic Ellipsometer

Slew rate for polarizer and analyzer azimuth	1.6°/ms to 0.33°/s
Dynamic range for analyzer azimuth	51°
Dynamic range for polarizer azimuth	55°
Resolution	7×10^{-4} to 8×10^{-2} deg
Cross-modulation for 5° azimuth change in one channel	<±0.002°
50° azimuth change in one channel	<±0.02°

FIGURE CAPTIONS

Fig. 1. Block diagram of self-nulling ellipsometer.

A	Analyzer
AF	Analyzer Faraday cell
C	Collimator
CT	Controller
DVM1	Digital voltmeter indicating polarizer rotation
DVM2	Digital voltmeter indicating analyzer rotation
F	Filter (λ = 546.1 nm)
G1	Galvanometer-oscillograph for polarizer rotation
G2	Galvanometer-oscillograph for analyzer rotation
L	High pressure mercury arc lamp
M1	Polarizer AC-power supply
M2	Analyzer AC power supply
O	Oscillator
P	Polarizer
PF	Polarizer Faraday cell
PM	Photomultiplier
PS1	Polarizer DC power supply
PS2	Analyzer DC power supply
Q	Compensator
S	Sample
T	Telescope

Fig. 2. Effect of azimuth modulation near extinction on output of photodetector with transfer characteristic T. (a) Azimuth modulation, (b) resulting modulation in photodetector output, (c) output after phase-sensitive detection, (d) output after integration (control signal).

1. Modulation around azimuth below compensation, resulting in a negative control signal.
2. Modulation around azimuth at compensation, resulting in a zero control signal.
3. Modulation around azimuth above compensation, resulting in positive control signal.

Fig. 3. Faraday cell solenoids (cross-section).

A cooling water connections for DC coil

B electrical connections for DC coil

C temperature sensor on water exit-side of DC coil

D DC coil, with glass tape-epoxy insulation

E separation coil on 76 mm O.D. core

F AC coil on 25 mm O.D. core

G leads for AC coil

H solenoid flange, attached to core of decoupling coil

Fig. 4. Axial component of magnetic field strength in the Faraday cell core due to the DC solenoid, carrying 125 A. (a) Variation with distance Z along the axis (R=0) of the solenoid, (b) variation with radial distance R from the solenoid axis for different positions Z along the axis.

Fig. 5. Block diagram of controller circuit.

A1, A2	Amplifiers (gain 1-100×)
AD	Analyzer Faraday DC solenoid
AA	Analyzer Faraday AC solenoid
F	Follower (gain 10×)
Int 1 Int 2	Integrators (0.001-0.5s)
I1, I2	Inverting operational amplifiers
L1, L2	Phase sensitive detectors
LD	Level Detector
M1, M2	Modulation amplifiers
O	Oscillator
PD	Polarizer Faraday DC solenoid
PA	Polarizer Faraday AC solenoid
PM	Photomultiplier
PS1, PS2	DC power supplies (with manual current controls)
QC	Quadrature circuit
SWG1, SWG2	Square wave generators
TA	Tuned amplifier
TD1, TD2	Multivibrators (with phase adjustments)

Fig. 6. Components of self-nulling ellipsometer.

A	analyzer prism with azimuth circle and telescope, on base with alignment facilities
AF	analyzer Faraday cell, on base with alignment facilities
F	monochromatic filter

L light source, on base with alignment facilities

P polarizer prism with azimuth circle and collimator, on base with alignment facilities

PF polarizer Faraday cell, on base with alignment facilities

PM photomultiplier housing

Q quarter wave plate compensator, with azimuth circle on base with alignment facilities

S specimen surface (in flow channel)

SI base plate of incident-light subassembly

SR base plate of reflected-light subassembly

Electronic rack at left (top to bottom): high voltage power supply for photomultiplier; control of scale illumination; controller with panel meters for error signal; digital voltmeters for azimuth readout; DC power supply for polarizer Faraday cell with current meter; same for analyzer; cooling water valves. Electronic rack at right (top to bottom): lamp power supply; modulation amplifiers for polarizer and analyzer Faraday cells; galvanometer preamplifiers; galvanometer driver amplifiers; galvanometer light-beam oscillograph; power supplies for electrochemical experiments.

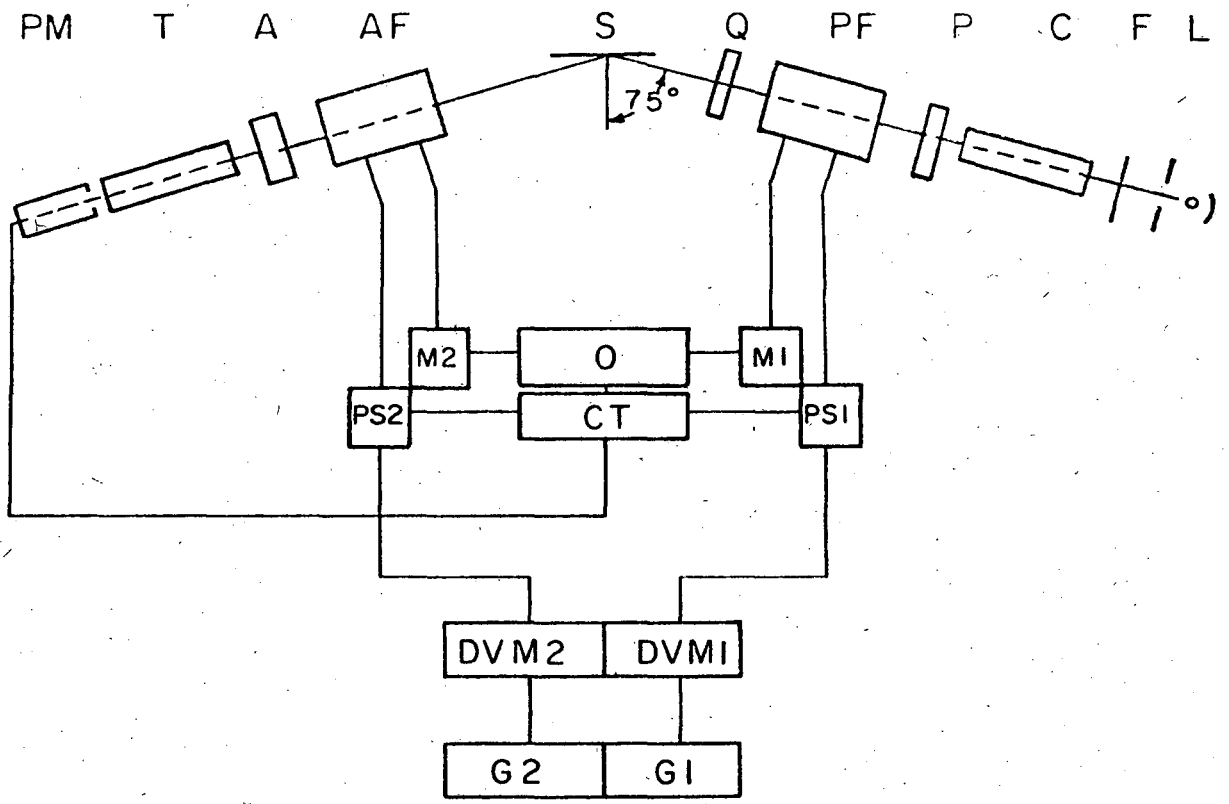

XBL7310 - 4210

Fig. 1

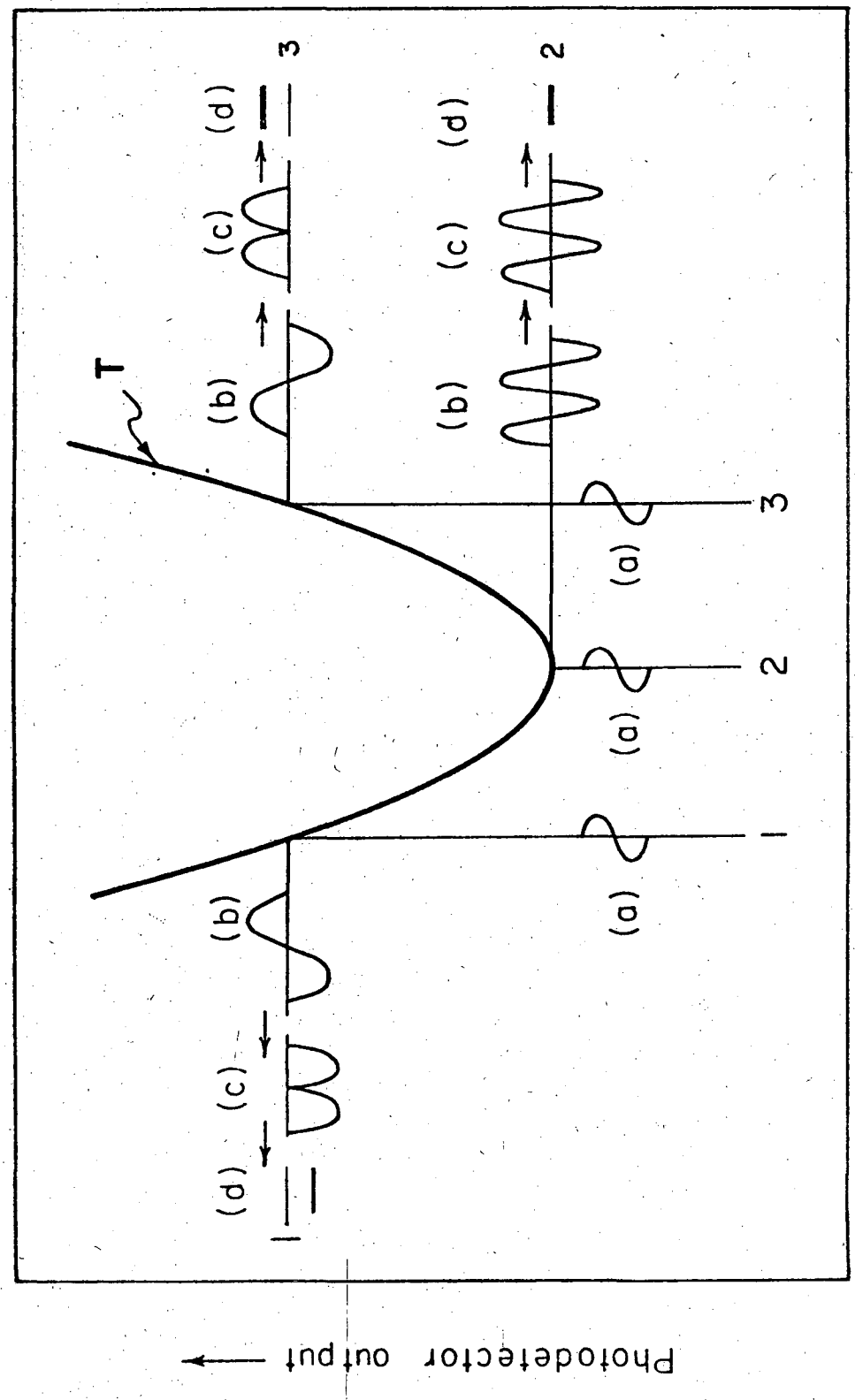

XBL7310-4207

Fig. 2

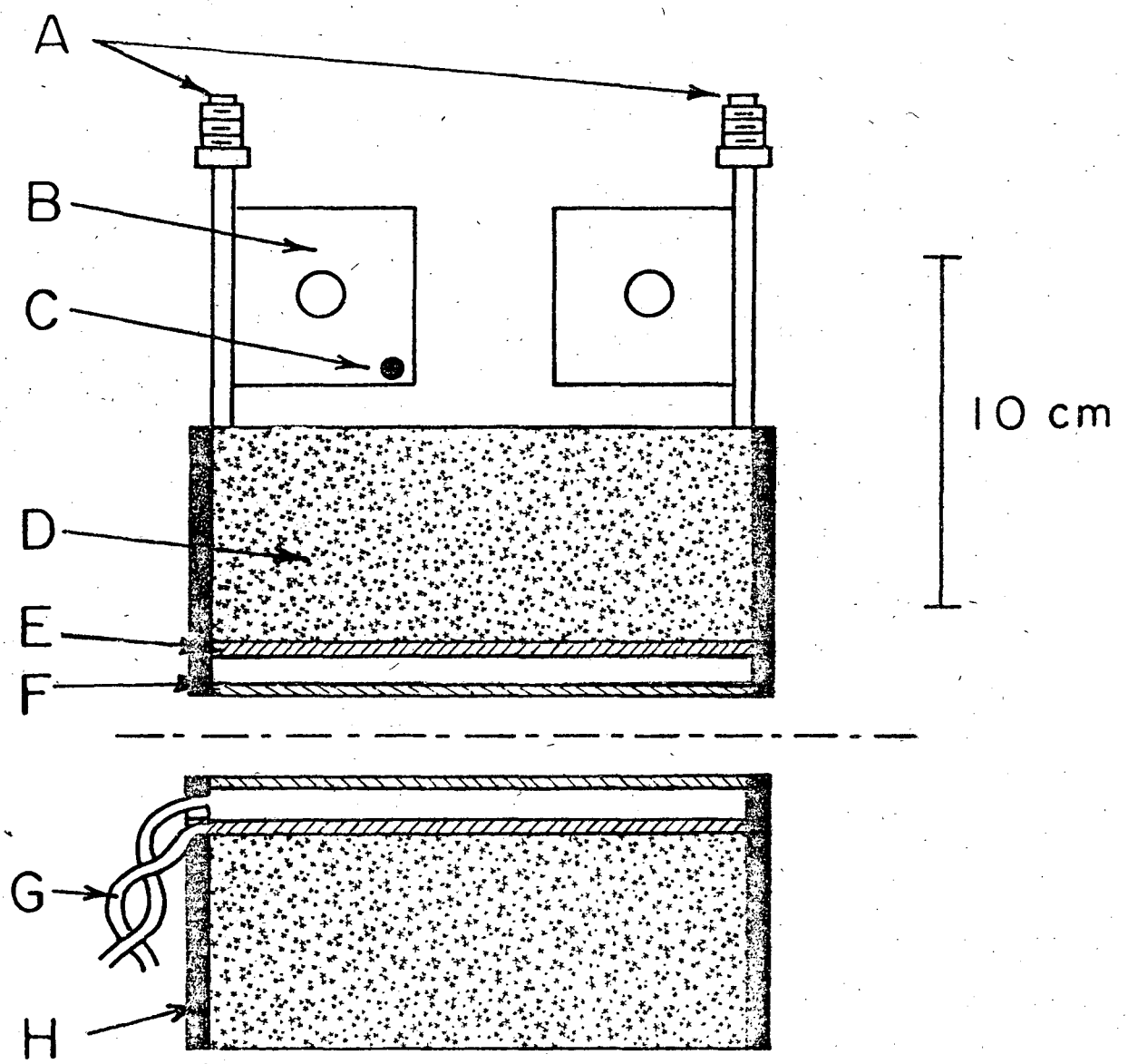

XBL 7310 - 4208

Fig. 3

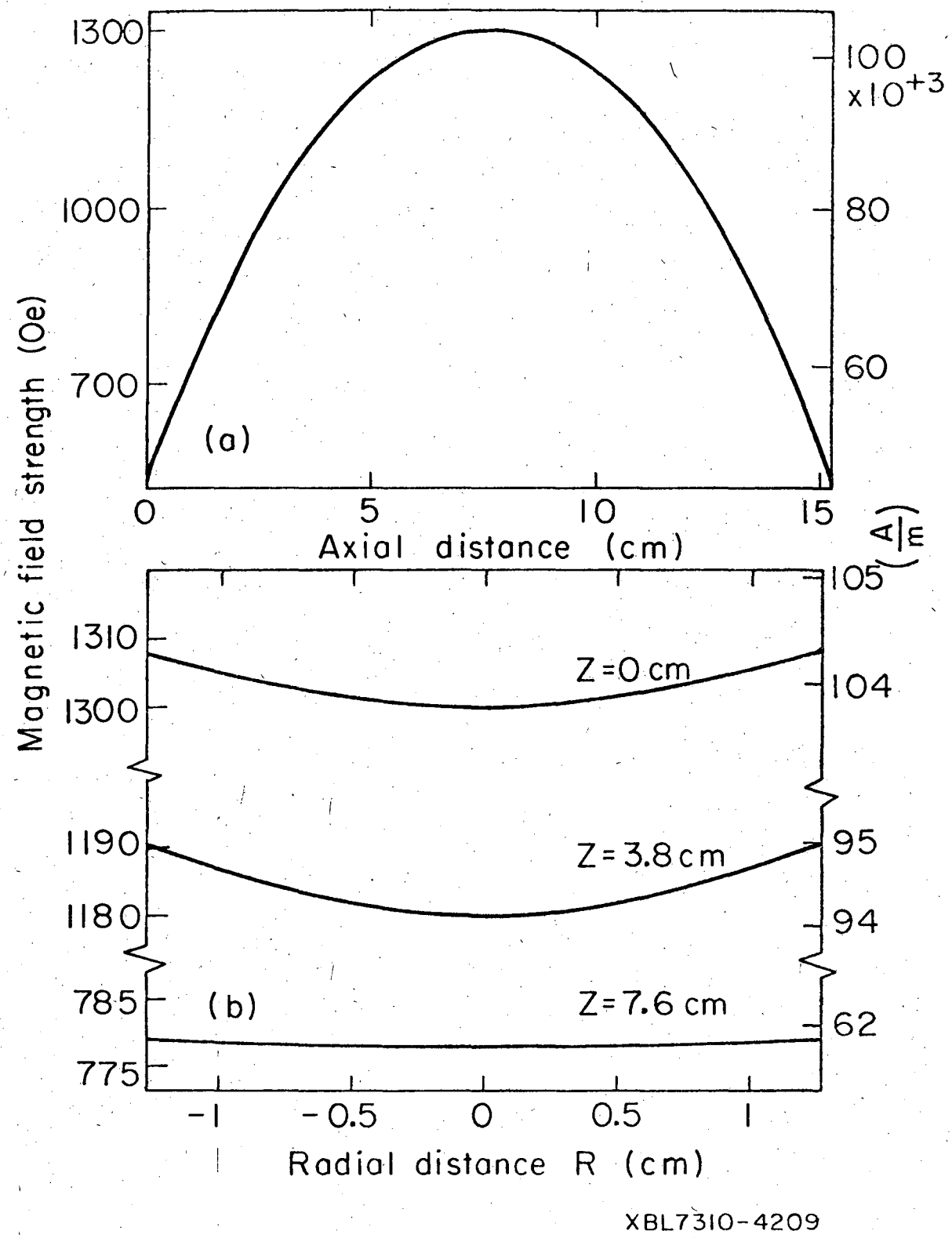
1300
1000
700
(a)
0
5
10
15
Axial distance (cm)
100
x10+3
80
60
Magnetic field strength (Oe)
(A/m)
105
1310
1300
Z=0 cm
104
1190
1180
Z=3.8 cm
95
94
785
775
(b)
Z=7.6 cm
62
-1
-0.5
0
0.5
1
Radial distance R (cm)
XBL7310-4209

Fig. 4

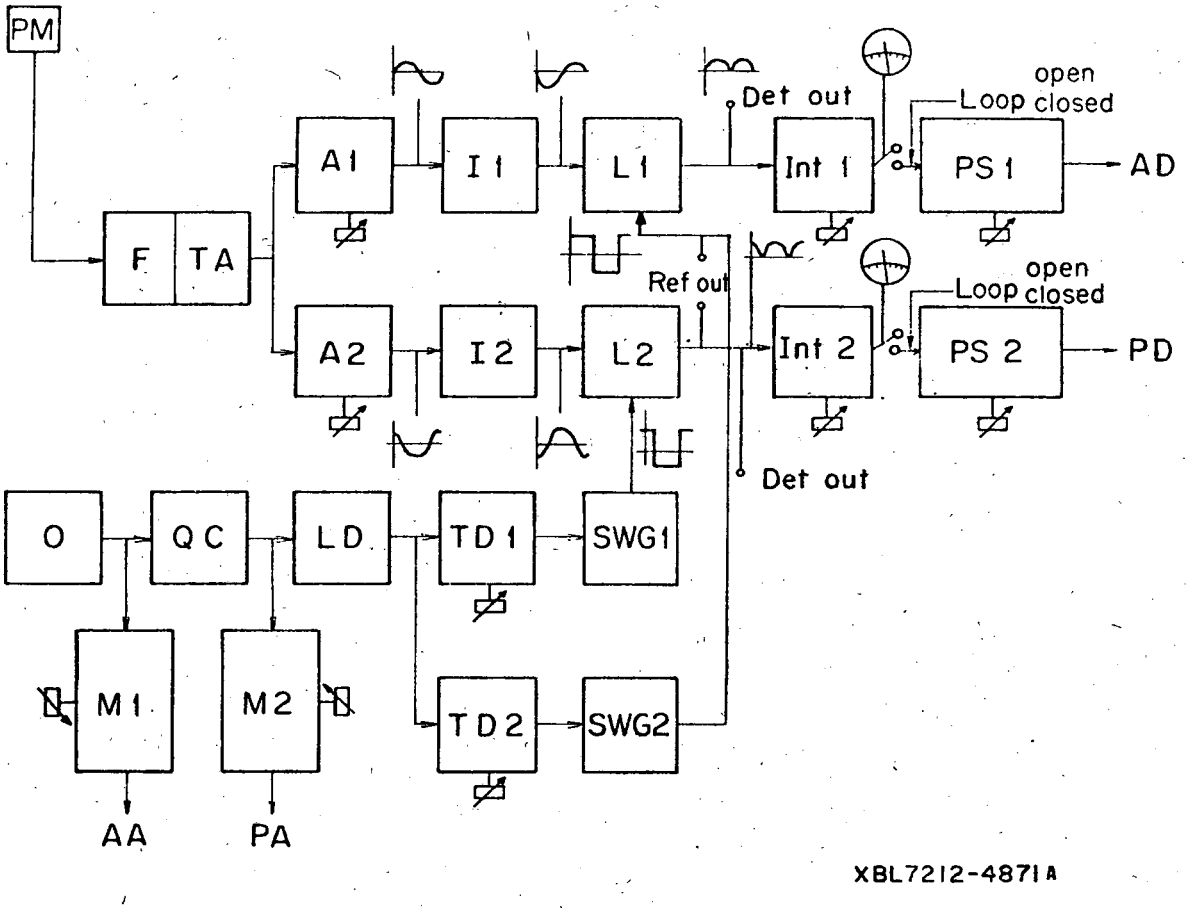
PM
F
TA
A1
I1
L1
Det out
Int 1
open
Loop closed
PS 1
AD
Ref out
A2
I2
L2
Int 2
PS 2
PD
Det out
O
QC
LD
TD1
SWG1
M1
M2
TD2
SWG2
AA
PA
XBL7212-4871A

Fig. 5

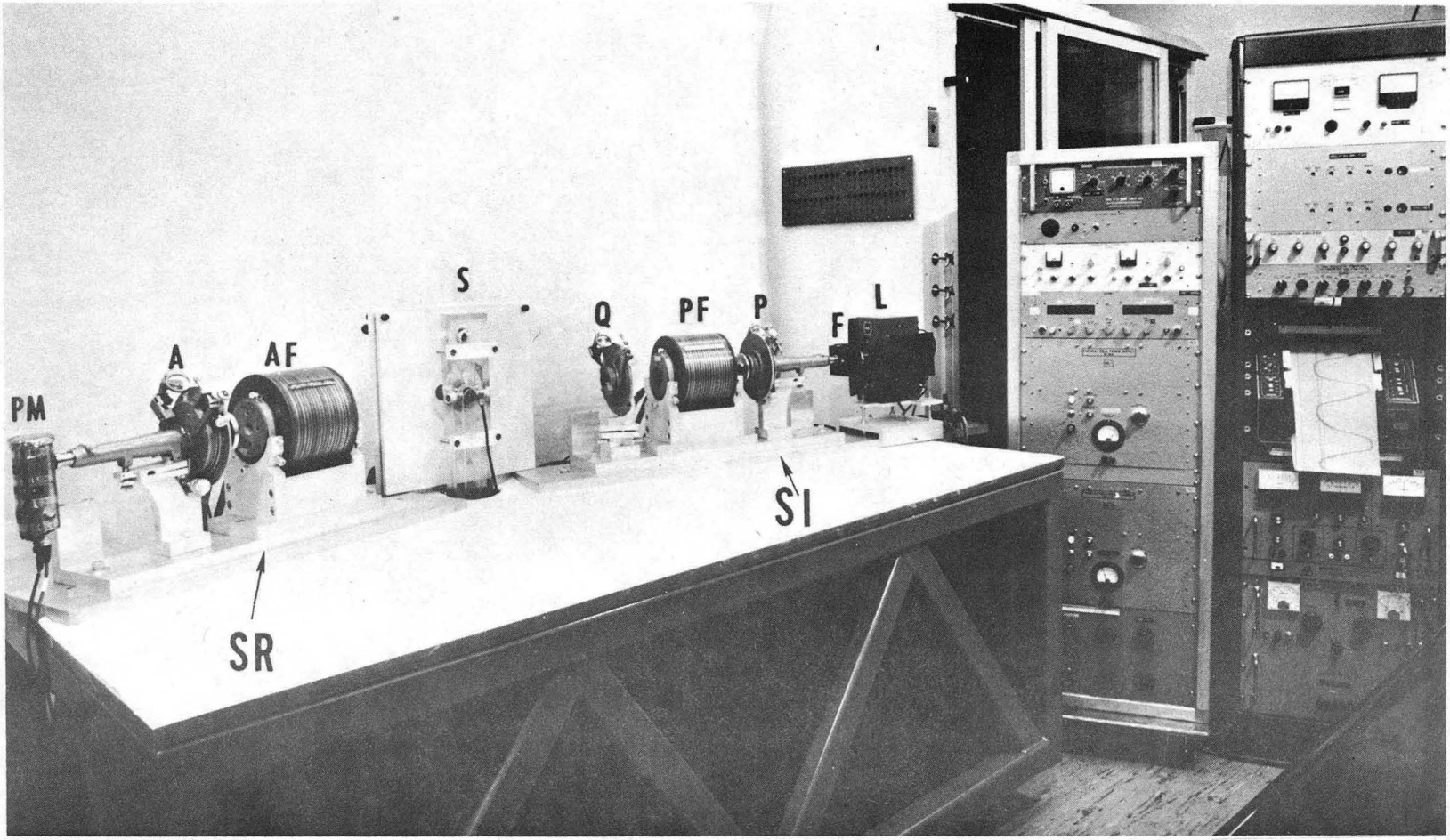

XBB 7311-4396A

Fig. 6

TECHNICAL INFORMATION DIVISION
LAWRENCE BERKELEY LABORATORY
UNIVERSITY OF CALIFORNIA
BERKELEY, CALIFORNIA 94720